



Syntheses, structural characterization and in vitro cytotoxic activity of triorganotin(IV) complexes based on 1,7-dihydroxycarbonyl-1,7-dicarba-closo-dodecaborane ligand

Huaiwei Wang, Dacheng Li, Min Hong*, Jianmin Dou*

Shandong Provincial Key Laboratory of Chemical Energy Storage and Novel Cell Technology, School of Chemistry and Chemical Engineering, Liaocheng University, Liaocheng 252059, China

ARTICLE INFO

Article history:

Received 21 February 2013

Received in revised form

19 April 2013

Accepted 25 April 2013

Keywords:

Organotin(IV)

1,7-Dihydroxycarbonyl-1,7-dicarba-closo-dodecaborane

X-ray crystallography

In vitro cytotoxic activity

ABSTRACT

Seven novel triorganotin(IV) compounds containing $m\text{-CDC}^{2-}$ ($m\text{-CDCH}_2 = 1,7\text{-dihydroxycarbonyl-1,7-dicarba-closo-dodecaborane}$) have been synthesized and structural characterized. The central tin atoms are five-coordinated to assume a distorted trigonal bipyramidal configuration not only in the binuclear monomers **1**, **3** and **4** but also in the polymers **2**, **5**, **6** and **7**. It was observed that complexes **3**, **4** and **5** could be obtained only in the presence of the ancillary carboxylate ligands, 2,3-pyrazinedicarboxylic acid, 2-pyridinecarboxylic acid and 2,6-pyridinedicarboxylic acid, respectively. The reaction of $m\text{-CDCH}_2$ with $(n\text{-Bu}_3\text{Sn})_2\text{O}$ in the presence of the bridging ligands 4,4'-bipyridine and 4,4'-vinylenedipyridine afforded one-dimensional coordination polymers **6** and **7**, respectively. Most of the complexes exhibit higher cytotoxic activities than cis-platin against two cancer cell lines, K-562 and Hela.

© 2013 Elsevier B.V. All rights reserved.

1. Introduction

Cisplatin and other platinum species belong to the blockbusters of anticancer drug sold worldwide. However, remaining problems such as severe side effects and resistance phenomena trigger an increasing demand for novel innovative drugs with a mode of action differing from that of the platinum generation of cancer chemotherapeutics [1–3]. In recent years especially, organotin(IV) complexes have attracted major attention due to their structural variety (ranging from monomer to polymer, from linear to pentagonal-bipyramid and even beyond) [4] and far more diverse stereochemistry than platinum derivatives, and by rational ligand design, provide control over key kinetic properties (such as hydrolysis rate of ligands) [5]. Furthermore, they are kinetically stable and relatively lipophilic. Because of these fundamental differences compared to “classical coordination metal complexes”, organotin(IV) complexes offer ample opportunities in the design of novel classes of medicinal compounds, potentially with new metal-specific modes of action [1,6,7]. Interestingly, many highly promising results with novel

organotin(IV) species have been reported, shedding more light on the issue of drug design.

The polyhedral boron clusters “carboranes” have extensive applications in the pharmaceuticals (such as for boron neutron capture therapy) [8–11]. A series of amine-carboxyboranes and polyhedral hydroborate salts were tested for their anti-neoplastic-cytotoxic activity [12–15]. Hall et al. observed that a number of compounds exhibited cytotoxicity in single cell suspended tumors (leukemia and Hela-S³) and not surprisingly, the substituents off the carboranes dramatically influenced the observed ED₅₀ values in a given screen. However, in general, they were not as potent as metal complexes with copper, cobalt, iron or chromium derivatives [16–18] or the heterocyclic amine-carboxyboranes [19].

Several carboxylate derivatives of tin based on 1,2- or 1,7-dicarba-closo-dodecaborane have also been reported [20–24], in which the carborane cage is linked to the carboxylic moiety via a boron or carbon atom. Studies reveal that these carborane-based organotin compounds present lower in vitro antitumor activities than the clinically used methotrexate and doxorubicin, but higher than 5-fluorouracil, cis-platin and carboplatin. Currently, the best known and most investigated carboranes are the three 12-vertex ortho, meta, and para isomers C₂B₁₀H₁₂, dicarbo-closo-dodecaboranes. Here, we first report the syntheses, characterization and in vitro cytotoxic activities of a series of novel triorganotin dicarboxylate derivatives of 1,7-dihydroxycarbonyl-1,7-dicarba-closo-

* Corresponding authors. Tel.: +86 635 8239795, +86 635 8230662; fax: +86 635 8239001.

E-mail addresses: hongminlcu@163.com (M. Hong), dougroup@163.com (J. Dou).

dodecaborane. It is expected that the biological activities of organotin(IV) compounds could be enhanced by the introduction of carborane, which would afford more opportunities for designing new antitumor drugs with higher activity.

2. Results and discussion

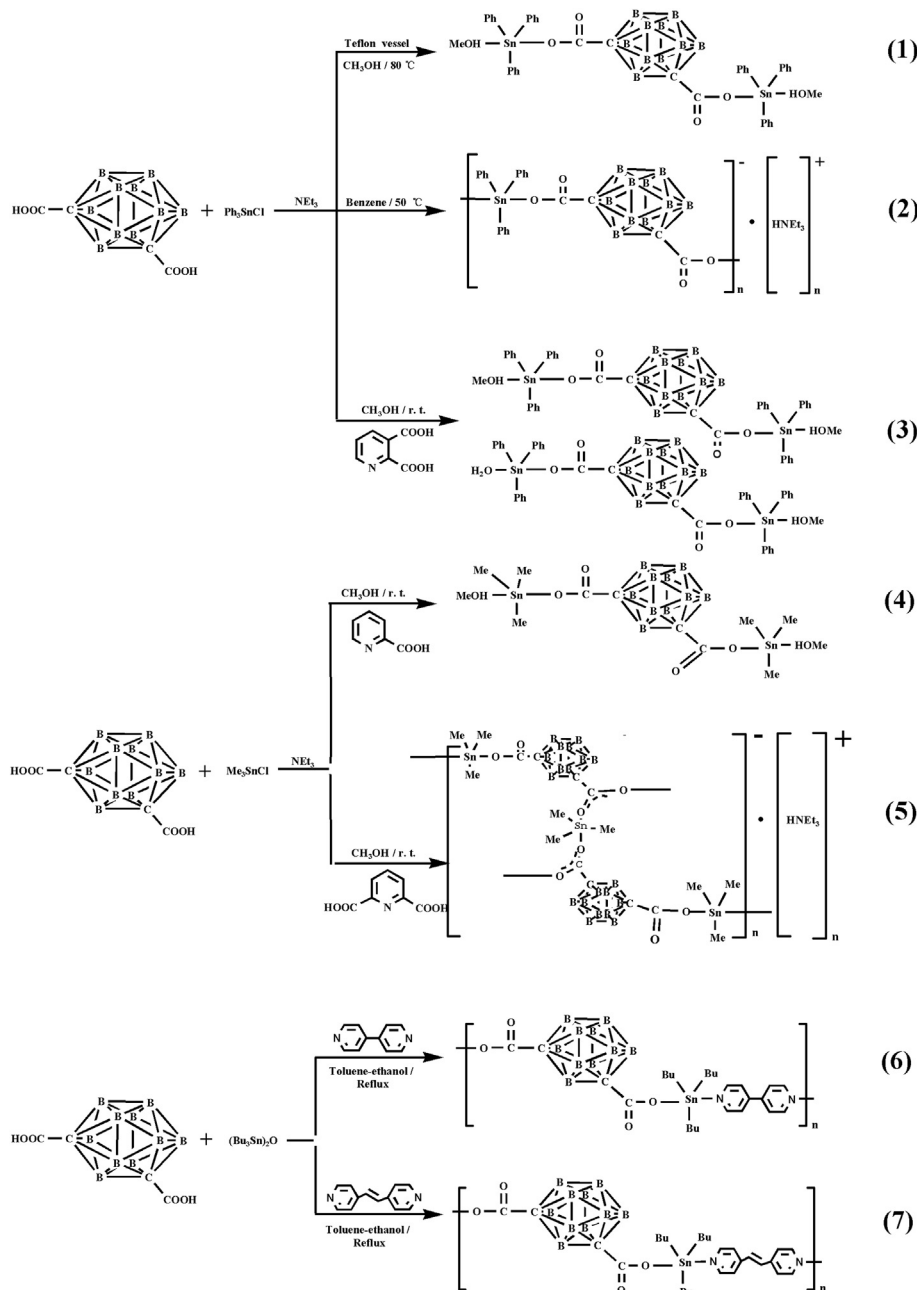
2.1. Syntheses

All complexes were prepared with different methods under atmospheric conditions. Complexes **1–6** are colorless crystals, and complex **7** is a light red crystalline solid. All compounds except for complex **2** are stable in air. It is interesting that complexes **3–5** can be obtained in the presence of the ancillary carboxylic acid ligands, 2,3-pyrazinedicarboxylic acid, 2-pyridinecarboxylic acid or 2,6-pyridinedicarboxylic acid, respectively, which are not involved in

the coordination of organotin(IV) compounds. We failed to obtain complexes **3–5** when the reactions were carried out in the absence of the ancillary ligands. About this phenomenon, it may result from the adjustment of the pH values by adding the ancillary carboxylic acids, which may be favorable to the formation of carborane carboxylate organotin(IV) compounds. Meanwhile, the carborane carboxylic acid may have a higher competitiveness than the ancillary ligand due to its earlier into the chemical reaction, and the specific reason is unclear. The synthesis procedures of complexes **1–7** are summarized in Scheme 1.

2.2. IR spectra

The IR spectra of complexes **1–7** were recorded in the range of 4000–400 cm^{-1} . The stretching frequencies of interest are those associated with COO^- , Sn-C , Sn-N and Sn-O groups. The strong



Scheme 1. The reaction procedures.

absorption in the region 430–490 cm^{-1} , which is absent in the spectrum of the free ligand, is assigned to the Sn–O stretching mode. Also, the strong absorption bands that appear at 1600–1670 cm^{-1} and 1330–1390 cm^{-1} in these spectra are assigned to the asymmetric and symmetric vibrations of the COO^- moiety, respectively. All these values are consistent with those detected in a number of organotin(IV)-oxygen derivatives [25].

2.3. NMR spectra

The ^1H NMR spectra show that the signals of the $-\text{CO}_2\text{H}$ proton in the spectrum of the ligands are absent in these complexes, indicating the removal of the $-\text{CO}_2\text{H}$ proton and the formation of Sn–O bond. The information well accords with what the IR data have revealed. The ^{13}C NMR spectra of all complexes show a significant downfield shift of all carbon resonances compared with the free ligands because of an electron-density transfer from the ligands to the metal atoms. The single resonance at $\delta = 165.78$ –166.99 ppm are attributed to the COO^- groups in complexes 1–7. These data are consistent with the structures of 1–7.

^{119}Sn NMR chemical shifts of tin complexes appear to depend on not only the coordination number, but also the type of donor atoms bonding to the metal ion. The δ values for ^{119}Sn NMR chemical shift may be used to give tentative indications of the coordination environment around tin atoms in the solution. The δ values for ^{119}Sn NMR chemical shifts of triphenyltin complexes 1–3 exhibit a single sharp resonance at -86.5 ppm, -99.6 ppm and -85.5 ppm, respectively, which are consistent with the range for tetrahedral geometry [20,26]. The ^{119}Sn NMR chemical shifts show a single resonance at 172.17 and 162.97 ppm for trimethyltin(IV) complexes 4 and 5, and for tributyltin(IV) compounds 6 and 7 at 146.50 and 143.41 ppm, all of which are characteristic of the four-coordinated triorganotin(IV) compounds [27]. Obviously, solution ^{119}Sn NMR spectra of these compounds are different from the five-coordinated tin centers determined by the X-ray crystal structural analysis, especially for coordination polymers 5–7. For compounds 1–5, the collapse of the intermolecular interactions existing in the solid state could result from the rupture of the weaker Sn–O bond with longer bond length observed in their crystal structures. These weaker Sn–O bonds are formed by the R_3Sn moiety and the coordinated solvent molecules MeOH or H_2O in compounds 1, 3 and 4, or by the R_3Sn moiety and the carboxyl group in compounds 2 and 5. But for compounds 6 and 7, the bond length of Sn–N [2.527(6) Å, 2.564(6) Å and 2.528(7) Å] determined by X-ray crystal diffraction is longer than that of the conventional Sn–N bonds, such as in the triorganotin(IV) pyridinecarboxylates, at about 2.2–2.3 Å [28], and the rupture of Sn–N bonds results in the four-coordinated triorganotin(IV) monomeric species in the solution.

2.4. Description of crystal structures

2.4.1. Crystal structures of complexes 1, 3 and 4

For these three complexes, the molecular structures are illustrated in Figs. 1–3, respectively; selected bond lengths and bond angles for these complexes are given in Table 1. They are all discrete molecules and have similar structures. Complex 1 is a discrete binuclear structure. Complexes 3 and 4 both own two monomers in a crystal unit. Two kinds of monomers in complex 3 are different due to one water molecule coordinated to Sn(2), which is different from the coordination environment of the other tin atoms in complex 3. In contrast to this, the structures of two monomers in complex 4 are the same. The geometries around Sn atoms in these complexes are trigonal bipyramidal with the axial positions being occupied by two oxygen donor atoms from the carboxylate and the methanol or water molecule. The equatorial planes were taken up

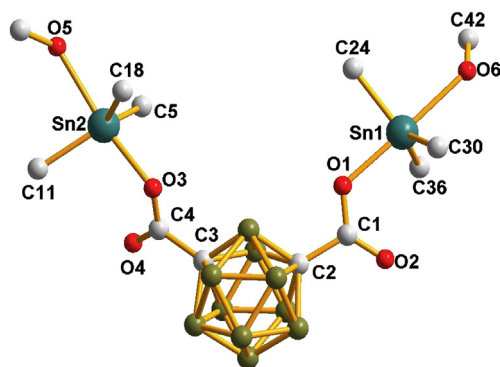


Fig. 1. Molecular structure of complex 1 (the additional carbon atoms of the Sn-Phenyl groups are omitted for clarity).

by three phenyl groups (1 and 3) or three methyl groups (4). The mean axial angles O–Sn–O, 173.1° (1), 175.8° (3) and 175.7° (4), suggest that these structures are nearly ideal trigonal bipyramid. Two types of Sn–O bonds are present in these complexes: a short distance ranging from 2.151 Å to 2.219(18) Å and a longer distance lying in the range of 2.376–2.50 Å, which are close to that reported in other triorganotin carboxylates [29,30].

In their supramolecular structures, the tin-coordinated methanol molecules and the water molecules play a crucial role, since each of them participates in an intermolecular hydrogen bond with oxygen atom of the carboxylate group in their structures. For complexes 1 and 3, the discrete molecules can form the 2D network supramolecular structures (Supporting information, Fig. S1 for 1 and Fig. S2 for 3) via $\text{O}-\text{H}\cdots\text{O}=\text{C}$ intermolecular hydrogen-bonding interactions (shown in Table 2). In complex 4, the two monomers interact with each other via hydrogen-bonding interactions to form a 20-membered hydrogen-bonding ring and a 44-membered hydrogen-bonding ring, resulting in the construction of supramolecular network together (Fig. S3).

2.4.2. Crystal structures of complexes 2 and 5

Both complexes 2 and 5 are ionic compounds, in which the organotin(IV) carboxylate anions are counteracted by the triethylammonium cations. The repeating unit, the 1D infinite chain and

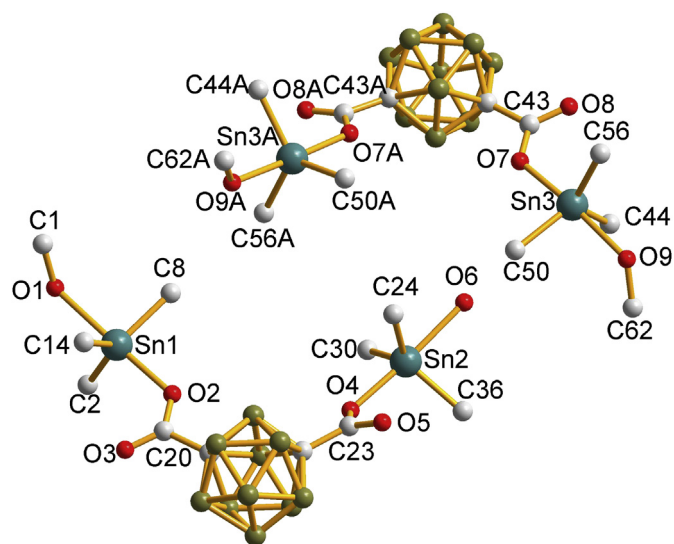


Fig. 2. Molecular structure of complex 3 (the additional carbon atoms of the Sn-Phenyl groups are omitted for clarity).

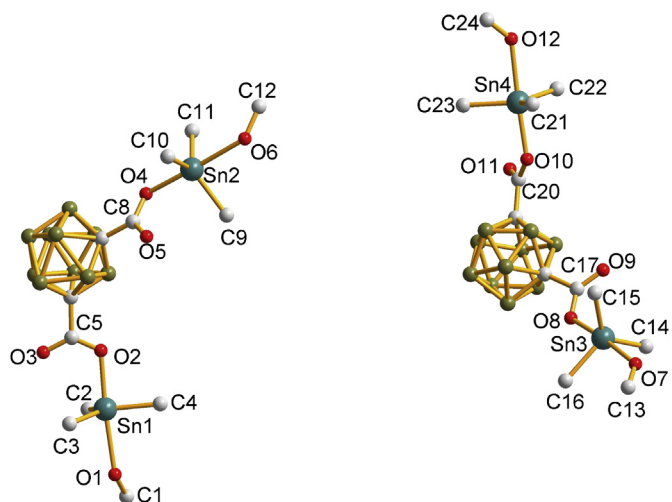


Fig. 3. Molecular structure of complex 4.

the 2D supramolecular structure of complex 2 are illustrated in Figs. 4 and 5 and Fig. S4, respectively. The repeating unit, the ladder-shaped structure and the 3D supramolecular structure of complex 5 are shown in Figs. 6 and 7 and Fig. S5, respectively. Selected bond lengths and bond angles for these complexes are listed in Table 3. In complex 2, the dicarboxylate ligand acts a connector and binds two successive triphenyltin atoms, which results in the formation of the 1D chain. In complex 5, the trimethyltin(IV) groups are linked by the deprotonated *m*-CDCH₂ ligand, which affords the formation of 1D chain. Further, two chains are connected along the opposite direction by the bidentate carboxylates coordinating to the trimethyltin(IV) groups, which gives rise to a ladder-shaped structure. As can be seen from Fig. 7, four ligands are linked by four metal centers into a 24-membered macrocycle, with a sort of cavity with width of 7.795 Å–10.678 Å.

In complexes 2 and 5, tin atom is trigonal bipyramidal (C₃O₂ coordination environment), with the apical positions being taken up by the oxygen atoms of two different deprotonated *m*-CDCH₂ ligands. The average of apical angle O–Sn–O of complexes 2 and 5 are 179.03° and 177.6°, respectively, which suggests that the structures are near to an ideal trigonal bipyramid. In complex 2, there exists only one type of Sn–O bond with the distance of 2.234(4) Å and 2.246(4) Å, and in complex 5, the distances of Sn–O bond range from 2.154 Å to 2.461 Å, which are close to those reported in other triorganotin carboxylates [31–33].

Analyses of the supramolecular structures in the crystal lattice of complexes 2 and 5 reveal that the triethylammonium cations play important roles in the supramolecular arrangements. The

Table 2
Hydrogen bonding geometries for complexes 1–6.

D–H···A	<i>d</i> (H···A)	<i>d</i> (D···A)	∠(DHA)
Complex 1			
O(6)–H(60)···O(2)#1	2.05	2.701(10)	135.5
O(5)–H(5A)···O(4)#2	1.88	2.645(9)	155.5
Complex 2			
N(1)–H(1A)···O(4)#3	1.91(11)	2.798(10)	164(9)
Complex 3			
O(1)–H(1)···O(5)#2	1.99	2.654(12)	138.0
O(6)–H(6A)···O(3)#3	1.88	2.726(12)	173.4
O(9)–H(90)···O(8)#4	1.87	2.656(13)	159.9
Complex 4			
O(1)–H(1E)···O(9)#1	1.80	2.62(3)	171.8
O(6)–H(6A)···O(11)#2	1.85	2.66(3)	167.1
O(7)–H(7C)···O(3)#3	1.80	2.61(3)	170.1
O(12)–H(12D)···O(5)#4	1.87	2.66(3)	164.3
Complex 5			
N(1)–H(1A)···O(6)#3	1.96(19)	2.84(2)	163(12)
Complex 6			
C(37)–H(37)···O(4)#3	2.27	3.094(9)	148.0

Symmetry code: (#1 for 1) $-x+1, y+1/2, -z+1/2$; (#2 for 1) $-x, y+1/2, -z+1/2$; (#3 for 2) $-x+2/3, -y+4/3, -z+1/3$; (#2 for 3) $x-1/2, y+1/2, z$; (#3 for 3) $x+1/2, y+1/2, z$; (#4 for 3) $-x+3/2, y-1/2, -z+1/2$; (#1 for 4) $x-1/2, -y+1/2, z+1$; (#2 for 4) $x, y, z+1$; (#3 for 4) $x, y-1, z-1$; (#4 for 4) $x+1/2, -y+1/2, z-1$; (#3 for 5) $x, y-1, z+1$; (#3 for 6) $x, y+1, z$.

triethylammonium cations, (Et₃NH)⁺, link two chains by the intermolecular N–H···O and C–H···O hydrogen-bonding interactions resulting in the formation of supramolecular structures of complexes 2 and 5 (Fig. S4 for 2 and Fig. S5 for 5).

2.4.3. Crystal structures of complexes 6 and 7

The X-ray crystal structures of 6 and 7, which are both 1D coordination polymers, are shown in Fig. 8a and b, respectively. The salient metric parameters of 6 and 7 are summarized in Table 4. In these complexes the dominant structure-directing role appears to be that of the ancillary ligand which alternates with the dicarboxylate ligands in a bridging coordination mode to form chain structures. The coordination polymers 6 and 7 represent interesting examples comprised of three distinct building blocks: (a) two tributyltin units; (b) a carboranedicarboxylate that bridges the two tin units and (c) a ditopic ligand containing two terminal nitrogen donor centers that interconnect the Sn₂/*m*-CDC motifs. The geometry around tin is a trigonal-bipyramid, where the equatorial positions are occupied by three *n*-butyl groups and the axial positions are shared by an oxygen donor atom from the carboxylate ligand and a nitrogen donor atom from the pyridine ligand. The mean Sn–N bond lengths for 6 and 7 are 2.546 Å and 2.528 Å, respectively, which are consistent with those reported in other triorganotin carboxylates [34].

Table 1
Selected bond lengths [Å] and angles [°] for complexes 1, 3 and 4.

1		3		4	
Sn(1)–O(1)	2.153(7)	Sn(1)–O(2)	2.173(8)	Sn(1)–O(1)	2.494(19)
Sn(1)–O(6)	2.424(7)	Sn(1)–O(1)	2.413(8)	Sn(1)–O(2)	2.219(18)
Sn(2)–O(3)	2.161(6)	Sn(2)–O(4)	2.150(8)	Sn(2)–O(6)	2.50(2)
Sn(2)–O(5)	2.417(6)	Sn(2)–O(6)	2.392(8)	Sn(2)–O(4)	2.182(17)
O(1)–Sn(1)–O(6)	176.1(3)	Sn(3)–O(7)	2.151(9)	Sn(3)–O(8)	2.167(18)
O(3)–Sn(2)–O(5)	170.1(2)	Sn(3)–O(9)	2.376(9)	Sn(3)–O(7)	2.40(2)
		O(4)–Sn(2)–O(6)	175.4(3)	Sn(4)–O(10)	2.169(18)
		O(2)–Sn(1)–O(1)	176.2(3)	Sn(4)–O(12)	2.41(2)
				O(2)–Sn(1)–O(1)	174.4(7)
				O(4)–Sn(2)–O(6)	176.7(8)
				O(8)–Sn(3)–O(7)	175.3(8)
				O(10)–Sn(4)–O(12)	176.2(7)

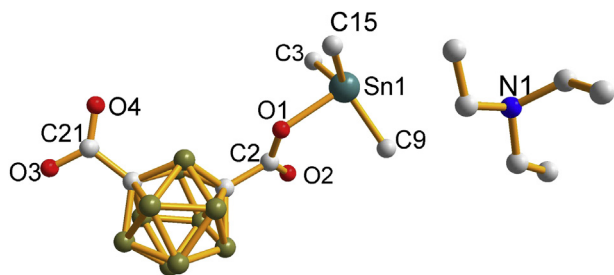


Fig. 4. Repeating unit of complex **2** (the additional carbon atoms of the Sn–Phenyl groups are omitted for clarity).

In their crystal structures, the 1D polymers of **6** interact with each other by two different C–H···O supramolecular interactions [C(10)–H(10B)···O(2) 3.334 Å] and [C(37)–H(37)···O(4) 3.094 Å]. The hydrogen atoms (H10B, H37) involved in C–H···O interactions belong to the butyl moiety and pyridine moiety, respectively, and the oxygen atoms (O2, O4) are derived from the deprotonated *m*-CDCH₂ ligand. Together, these interactions generate a 3D supramolecular architecture (Fig. S6a). The complex **7** is also a 1D coordination polymer whose structure is similar to that of **6**; however, its supramolecular assembly is different. Analysis of the supramolecular structure in the crystal lattice of **7** reveals that supramolecular interactions [C(20)–H(20)···O(2) 3.489 Å] (C20 derived from the pyridine ligand) play important roles in the supramolecular arrangements. The 1D polymers of **7** interact with each other via this interaction to form a 3D supramolecular structure (Fig. S6b).

2.5. In vitro cytotoxic activity

All compounds were screened for the preliminary in vitro cytotoxic activity studies on two different cell lines: chronic myeloid leukemia cell line (K562) and cervical cancer cell line (Hela), at five different concentrations ranging from 10 to 0.1 μM in DMSO. Relevant activities could be noted for all complexes in these two cell lines. The observed IC₅₀ values with the exception of complexes **1** and **3** due to their bad solubility are listed in Fig. 9. These results are in good agreement with other reports on bioactive organotin(IV) species, which reached activities in the low micromolar range [6,7,20].

Because most of the complexes showed inhibition activity at concentration of >10 μM, we herein merely listed biological results at concentration of 10 μM in Table 5 for the sake of discussing the structure–activity relationship. But for complexes **1** and **3**, owing to the partially solubility in DMSO, the top clear solution of the prepared 10 μM samples were used to determine their in vitro cytotoxicity. The inhibition [%] of triphenyltin(IV) complexes **1** and **3** at the unknown concentration (<<10 μM) against human tumor cells are listed in Table 6.

The results of in vitro cytotoxic effects demonstrate these complexes are active against two tumor cell lines (K562 and Hela) and generally exhibit higher activity than cisplatin [35,36], the clinically widely used drug. Also, the inhibitory potencies of the



Fig. 5. 1D chain structure of complex **2** (the additional carbon atoms of the Sn–Phenyl groups are omitted for clarity).

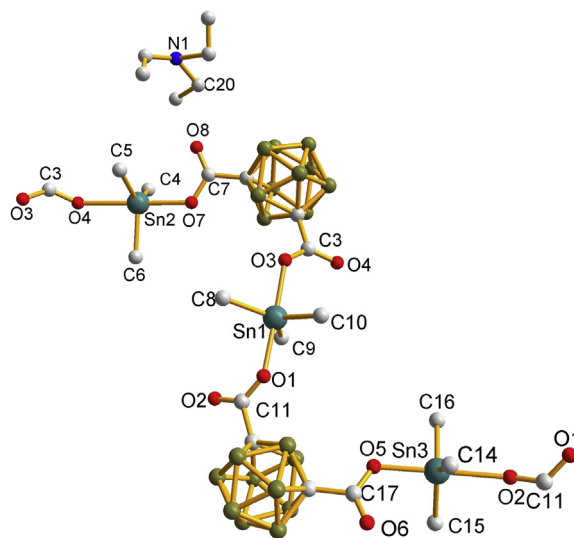


Fig. 6. Repeating unit of complex **5**.

same complex against different cell lines present a high selectivity. Generally, the higher activity is usually observed for the K-562 tumor cells and the lower one for the Hela tumor cells.

On the basis of the data analysis, possible structure–activity relationships could be outlined. According to the previous reports, the organo-ligand R bound with tin atom plays an important role for their biological activities [37,38], and usually in the condition of the same coordination structures, the anticancer activity of triorganotin(IV) complexes follows the trend of Bu > Ph > Me, which can also be proved in our present work, that is **2** > **5** for both two tumor cells. But for the different molecular structures, the in vitro cytotoxic activity would be influenced by several factors. For example, the triphenyltin derivative **2** exhibits higher activity than the tributyltin(IV) complexes **6** and **7**, which may be due to the form of zwitterion for complex **2** [39]. From the inhibition [%] of 10 μM samples we can also see that with the similar coordination environment, the triphenyltin complexes **1** and **3** are more active than the trimethyltin complex **4**.

Although both complexes **1** and **3** are low soluble, they exhibit higher activity compared with the other complexes. This encouraging cytotoxic activity may make complexes **1** and **3** be suitable candidates for further modification to improve their solubility which may influence the cytotoxicity. This research work is in progress in our laboratories.

Further chemical and pharmacological studies will be necessary to unravel a structure–activity relationship, from which novel organotin antitumor drugs with possible clinical applications can be developed.

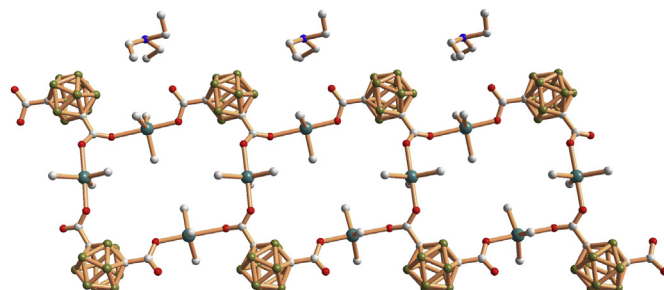


Fig. 7. Ladder-shaped structure of complex **5**.

Table 3
Selected bond lengths [Å] and angles [°] for complexes **2** and **5**.

2		5	
Sn(1)–O(3)	2.246(4)	Sn(1)–O(1)	2.236(7)
Sn(1)–O(1)	2.234(4)	Sn(1)–O(3)	2.250(7)
O(1)–Sn(1)–O(3)	179.03(15)	Sn(2)–O(7)	2.161(8)
		Sn(2)–O(4)	2.461(8)
		Sn(3)–O(2)	2.453(7)
		Sn(3)–O(5)	2.154(7)
		O(1)–Sn(1)–O(3)	176.9(4)
		O(7)–Sn(2)–O(4)	178.3(4)
		O(5)–Sn(3)–O(2)	177.5(3)

3. Conclusion

In conclusion, this contribution has shown that the reactions of *m*-CDCH₂ with triphenyl, trimethyl, and bis(tri-*n*-butyl)tin oxide moieties give either discrete or polymeric structures. The tin atoms in these complexes are Lewis acid and can form additional bonds to coordinating solvent molecules such as water, methanol molecule and pyridine.

It could be suggested that both the volume of the organic substituents attached to the tin atoms and the reaction solvent have an influence on the molecular structure and the supramolecular arrangement of the complexes. The reaction of *m*-CDCH₂ with triphenyltin chloride in the presence of methanol solvent afforded two discrete molecular compounds **1** and **3** while in the presence of aprotic solvents afforded the 1D chain complex **2**. In contrast to the reactions of *m*-CDCH₂ with triphenyltin, that involving trimethyltin chloride afforded a ladder coordination polymer **5** in the presence of 2,6-pyridinedicarboxylic acid, and complex **4** have a similar structure with complex **3** in the presence of 2-pyridinecarboxylic acid. If a third component is used in the reaction *m*-CDCH₂ with (*n*-Bu₃Sn)₂O in the form of the ancillary ligands, 4,4'-bipyridine and 4,4'-vinylenedipyridine, 1D coordination polymers **6** and **7** are obtained. In these two reactions the dominant structure-directing role appears to be that of the ancillary ligands which alternates

Table 4
Selected bond lengths [Å] and angles [°] for complexes **6** and **7**.

6		7	
Sn(1)–O(1)	2.170(5)	Sn(1)–O(1)	2.174(6)
Sn(1)–N(1)	2.527(6)	Sn(1)–N(1)	2.528(7)
Sn(2)–O(3)	2.184(5)	O(1)–Sn(1)–N(1)	176.3(2)
Sn(2)–N(2)	2.564(6)		
O(1)–Sn(1)–N(1)	172.08(19)		
O(3)–Sn(2)–N(2)	166.23(17)		

with the carboxylate ligand in a bridging coordination mode to form chain structures.

Complexes **2**, **4**, **5**, **6** and **7** display high in vitro cytotoxic activities against chronic myeloid leukemia cell line (K-562) and cervical cancer cell line (Hela). For the triorganotin(IV) complexes, the zwitterion triphenyltin derivatives **2** exhibit the highest activity. Therefore, we can see that the cytotoxic activity would be affected by both the organic ligand **R** and their molecular structures. Also, the methyltin compounds still show the lowest activity. The obtained results allow the recognition of preliminary structure–activity relationships, but the definite trend could yet be established. These bi- or multi-nuclear compounds with carborane ligand represent a new paradigm for tin-based antitumor complexes and appear to offer a great potential as new anticancer agents.

4. Experimental details

4.1. Materials and measurements

Triphenyltin chloride, trimethyltin chloride, bis(tri-*n*-butyl)tin oxide, triethylamine and solvents were commercially available and were used without further purification. The 1,7-dihydroxycarbonyl-1,7-dicarba-closo-dodecaborane was prepared according to the literature method [40]. The melting points were obtained with a Kofler micro melting point apparatus and are uncorrected. Elemental analyses were performed with a PE-2400II apparatus. Infrared spectra were recorded with a Nicolet-5700 spectrometer using KBr discs and NaCl optics. ¹H, ¹³C, and ¹¹⁹Sn NMR spectra were recorded with a Varian Mercury Plus 400 spectrometer operating at 400, 100.6, and 149.2 MHz, respectively. The spectra were acquired at room temperature (298 K), unless otherwise specified. The chemical shifts are reported in ppm with respect to the references and are stated relative to external tetramethylsilane (TMS) for ¹H

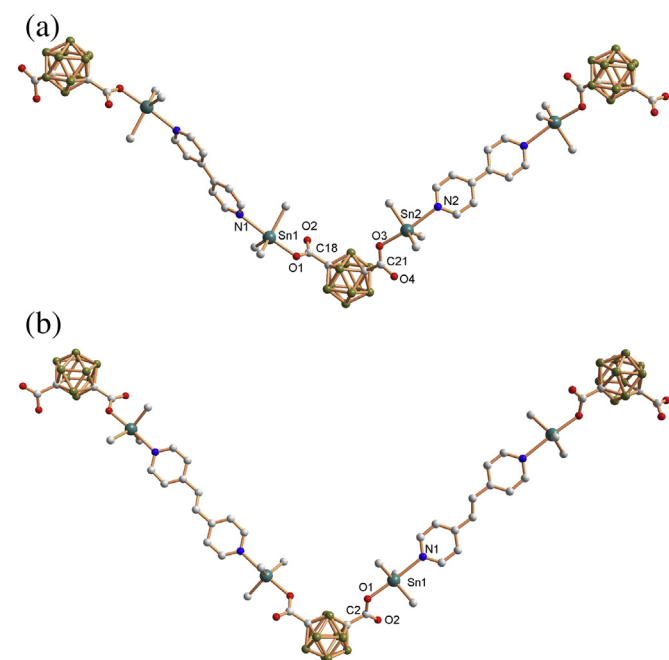


Fig. 8. (a) 1D polymeric structure of **6**. (b) 1D polymeric structure of **7** (the additional carbon atoms of the Sn–butyl groups are omitted for clarity).

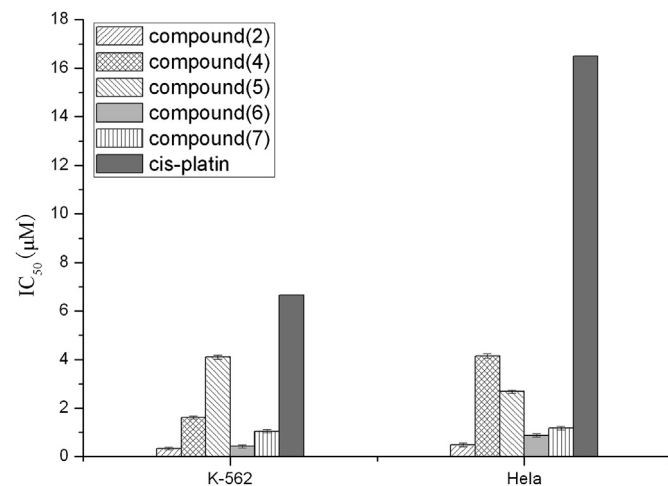


Fig. 9. In vitro cytotoxicity of complexes **2** and **4–7** against cancer cells K-562 and Hela. Data represent mean ± SD of three independent experiments.

Table 5Inhibition [%] of triorganotin(IV) complexes **2** and **4–7** [dose level of 10.0 μM] against human tumor cells.

NO	Compound	K-562	Hela
2	$\{[(\text{C}_2\text{H}_5)_3\text{NH}]^+ \cdot [(\text{Ph}_3\text{Sn})(m\text{-CDC})]^- \}_n$	85.65	84.41
4	$[(\text{Me}_3\text{Sn})_2(m\text{-CDC})(\text{CH}_3\text{OH})_2]$	69.39	65.30
5	$\{[(\text{C}_2\text{H}_5)_3\text{NH}]^+ \cdot [(\text{Me}_3\text{Sn})_3(m\text{-CDC})_2]^- \}_n$	73.98	68.83
6	$[(\text{Bu}_3\text{Sn})_2(m\text{-CDC})(4,4'\text{-bipy})]_n$	82.97	90.38
7	$[(\text{Bu}_3\text{Sn})_2(m\text{-CDC})(4,4'\text{-bpe})]_n$	82.91	77.67

and ^{13}C NMR and to neat tetramethyltin for ^{119}Sn NMR. The ^{13}C and ^{119}Sn NMR spectra were determined in the decoupling mode.

4.2. Syntheses of complexes **1–7**

4.2.1. $[(\text{Ph}_3\text{Sn})_2(m\text{-CDC})(\text{CH}_3\text{OH})_2]$ (**1**)

A mixture of *m*-CDCH₂ (23.2 mg, 0.10 mmol), triethylamine (0.2 mmol, 20.2 mg) and triphenyltin chloride (77.1 mg, 0.2 mmol) in 20 ml CH₃OH was sealed in a Teflon-lined bomb and heated to a temperature of 80 °C for 2 days, then cooled slowly to room temperature. The filtrate was allowed to evaporate slowly at room temperature. After two weeks colorless crystals suitable for X-ray diffraction were obtained. Yield: 82%. M.P. 154–156 °C. Anal. Calc. for C₄₂H₄₈B₁₀O₆Sn₂: C 50.73, H 4.87%; Found: C 50.45, H 5.02%. IR (KBr, cm⁻¹): $\nu_{\text{as}}(\text{COO})$, 1606.9; $\nu_{\text{s}}(\text{COO})$, 1384.4; $\nu(\text{Sn}-\text{C})$, 544; $\nu(\text{Sn}-\text{O})$, 453.8. ^1H NMR (CDCl₃, ppm): δ 3.49 (s, 6H, -CH₃), 1.26 (s, 2H, -OH), 7.62–7.66 (m, 30H, Ph). ^{13}C NMR (CDCl₃, ppm): δ 166.15 (COO); 128.26–136.80 (Ph-C); 76.61, 76.93 (C-1 and C-7); 50.52 (CH₃OH-C). ^{119}Sn NMR (CDCl₃, ppm): δ -86.5.

4.2.2. $\{[(\text{C}_2\text{H}_5)_3\text{NH}]^+ \cdot [(\text{Ph}_3\text{Sn})(m\text{-CDC})]^- \}_n$ (**2**)

The *m*-CDCH₂ (23.2 mg, 0.1 mmol) was added to the solution of benzene together with triethylamine (0.2 mmol, 20.2 mg), and the mixture was stirred for 10 min. After the addition of triphenyltin chloride (77.1 mg, 0.2 mmol), the mixture was reacted at 50 °C for 10 h and then filtered. The solvent was gradually removed by evaporation under vacuum until a solid product was obtained. The obtained solid was then recrystallized from dichloromethane/hexane (*v/v* = 3:1), and colorless crystals of complex **2** were recovered. Yield: 63%. M.P. 116–118 °C. Anal. Calc. for C₂₈H₄₁B₁₀N₄O₄Sn: C 49.28, H 6.06, N 2.05%; Found: C 48.99, H 6.22, N 2.19%. IR (KBr, cm⁻¹): $\nu_{\text{as}}(\text{COO})$, 1639.8; $\nu_{\text{s}}(\text{COO})$, 1349; $\nu(\text{Sn}-\text{C})$, 544.6; $\nu(\text{Sn}-\text{O})$, 455.4. ^1H NMR (CDCl₃, ppm): δ 1.24 (t, 9H, -CH₃), 3.02 (q, 6H, -CH₂), 7.64–7.66 (m, 15H, Ph). ^{13}C NMR (CDCl₃, ppm): δ 165.86 (COO); 128.979–136.00 (Ph-C); 76.60, 76.91 (C-1 and C-7). ^{119}Sn NMR (CDCl₃, ppm): δ -99.6.

4.2.3. $\{[(\text{Ph}_3\text{Sn})_2(m\text{-CDC})(\text{CH}_3\text{OH})_2] \cdot [(\text{Ph}_3\text{Sn})_2(m\text{-CDC})(\text{H}_2\text{O})(\text{CH}_3\text{OH})_2]\}_n$ (**3**)

m-CDCH₂ (23.2 mg, 0.10 mmol), and triethylamine (0.2 mmol, 20.2 mg) were dissolved in 20 ml CH₃OH. After 10 min the triphenyltin chloride (77.1 mg, 0.2 mmol) was added to the solution and then 2,3-pyrazinedicarboxylic acid (17.6 mg, 0.1 mmol) was added to the resulting solution after half an hour. The reaction was lasted 20 h and the filtrate was allowed to evaporate slowly at room

Table 6Inhibition [%] of triphenyltin(IV) complexes **1** and **3** at the unknown concentration [below dose level of 10.0 μM] against human tumor cells.

NO	Compound	K-562	Hela
1	$[(\text{Ph}_3\text{Sn})_2(m\text{-CDC})(\text{CH}_3\text{OH})_2]$	85.20	84.33
3	$\{[(\text{Ph}_3\text{Sn})_2(m\text{-CDC})(\text{CH}_3\text{OH})_2] \cdot [(\text{Ph}_3\text{Sn})_2(m\text{-CDC})(\text{H}_2\text{O})(\text{CH}_3\text{OH})_2]\}_n$	86.06	88.27

temperature. After three weeks the colorless block crystals were obtained. Yield: 71%. M.P. 125–127 °C. Anal. Calc. for C₁₂₄H₁₄₀B₃₀O₁₈Sn₆: C 50.40, H 4.78%; Found: C 50.16, H 4.97%. IR (KBr, cm⁻¹): $\nu_{\text{as}}(\text{COO})$, 1648.9; $\nu_{\text{s}}(\text{COO})$, 1384; $\nu(\text{Sn}-\text{C})$, 543.3; $\nu(\text{Sn}-\text{O})$, 453.1. ^1H NMR (CDCl₃, ppm): δ 3.46 (s, 12H, -CH₃), 1.46 (s, 4H, H₂O), 1.16 (s, 4H, -OH), 7.43–7.63 (m, 90H, Ph). ^{13}C NMR (CDCl₃, ppm): δ 166.16 (COO); 128.57–136.54 (Ph-C); 76.58, 76.90 (C-1 and C-7); 50.73 (CH₃OH-C). ^{119}Sn NMR (CDCl₃, ppm): δ -85.50.

4.2.4. $[(\text{Me}_3\text{Sn})_2(m\text{-CDC})(\text{CH}_3\text{OH})_2]$ (**4**)

m-CDCH₂ (23.2 mg, 0.10 mmol) and triethylamine (0.2 mmol, 20.2 mg) were dissolved in 20 ml CH₃OH. After 10 min the trimethyltin chloride (39.9 mg, 0.2 mmol) was added to the solution and then 2-pyridinecarboxylic acid (12.3 mg, 0.1 mmol) was added to the resulting solution after half an hour. The reaction was lasted 20 h and the filtrate was allowed to evaporate slowly at room temperature. After two weeks the colorless block crystals were obtained. Yield: 79%. M.P. 214–216 °C. Anal. Calc. for C₁₂H₃₆B₁₀O₆Sn₂: C 23.54, H 5.83%; Found: C 23.73, H 5.63%. IR (KBr, cm⁻¹): $\nu_{\text{as}}(\text{COO})$, 1631.3; $\nu_{\text{s}}(\text{COO})$, 1354.3; $\nu(\text{Sn}-\text{C})$, 555.2; $\nu(\text{Sn}-\text{O})$, 477.3. ^1H NMR (CDCl₃, ppm): δ 1.25 (s, 2H, -OH), 3.07 (s, 6H, -CH₃), 0.88 (s, 18H, Sn-CH₃). ^{13}C NMR (CDCl₃, ppm): δ 166.290 (COO); 8.19 (CH₃); 76.67, 76.87 (C-1 and C-7); 50.61 (CH₃OH-C). ^{119}Sn NMR (CDCl₃, ppm): δ 172.17.

4.2.5. $\{[(\text{C}_2\text{H}_5)_3\text{NH}]^+ \cdot [(\text{Me}_3\text{Sn})_3(m\text{-CDC})_2]^- \}_n$ (**5**)

m-CDCH₂ (23.2 mg, 0.10 mmol), and triethylamine (0.2 mmol, 20.2 mg) were dissolved in 20 ml CH₃OH. After 10 min the trimethyltin chloride (39.9 mg, 0.2 mmol) was added to the solution and then 2,6-pyridinedicarboxylic acid (16.7 mg, 0.1 mmol) was added to the resulting solution after half an hour. The reaction was lasted 20 h and the filtrate was allowed to evaporate slowly at room temperature. After three weeks the colorless block crystals were obtained. M.P. 208–210 °C. Yield. 61%. Anal. Calc. for C₂₃H₆₃B₂₀N₈O₈Sn₃: C 26.21, H 6.02, N 1.33%; Found: C 26.46, H 5.90, N 1.42%. IR (KBr, cm⁻¹): $\nu_{\text{as}}(\text{COO})$, 1623.6; $\nu_{\text{s}}(\text{COO})$, 1383.7; $\nu(\text{Sn}-\text{C})$, 545.4; $\nu(\text{Sn}-\text{O})$, 453.9. ^1H NMR (CDCl₃, ppm): δ 1.26 (t, 9H, -CH₃), 3.06 (m, 6H, -CH₂), 0.88 (s, 27H, Sn-CH₃). ^{13}C NMR (CDCl₃, ppm): δ 166.99 (COO); 8.28 (CH₃); 76.54, 76.86 (C-1 and C-7). ^{119}Sn NMR (CDCl₃, ppm): δ 162.97.

4.2.6. $[(\text{Bu}_3\text{Sn})_2(m\text{-CDC})(4,4'\text{-bipy})]_n$ (**6**)

A mixture of 0.10 mmol (*n*-Bu₃Sn)₂O, *m*-CDCH₂ (23.2 mg, 0.10 mmol) and 4,4'-bipy (19.2 mg, 0.10 mmol) was heated under reflux in a mixture of toluene and ethanol (10 ml, *v/v* = 3:2) for 6 h affording a clear solution. The reaction mixture was filtered and the solvent was removed in vacuo to afford a white solid product. The single crystals of **6** were obtained by the slow evaporation of CH₃CN/Acetone solution of product. Yield: 79%. M.P. 128–130 °C. Anal. Calc. for C₃₈H₇₂B₁₀N₂O₄Sn₂: C 47.22, H 7.51, N 2.90%; Found: C 47.52, H 7.31, N 2.71%. IR (KBr, cm⁻¹): $\nu_{\text{as}}(\text{COO})$, 1655.1; $\nu_{\text{s}}(\text{COO})$, 1383.7; $\nu(\text{Sn}-\text{C})$, 544.1; $\nu(\text{Sn}-\text{O})$, 464.9, $\nu(\text{Sn}-\text{N})$, 454.3. ^1H NMR (CDCl₃, ppm): δ 7.54 (d, 4H, bipy), 8.74–8.76 (d, 4H, bipy), 0.89–0.93 (t, 18H, butyl CH₃), 1.27–1.37 (m, 12H, butyl -CH₂-), 1.55–1.70 (m, 24H, butyl Sn-CH₂-CH₂-). ^{13}C NMR (CDCl₃, ppm): δ 165.78 (COO); 13.80, 17.11, 27.04, 27.74 (butyl-C); 76.57, 76.89 (C-1 and C-7); 150.57, 145.73, 121.59 (bipy-C). ^{119}Sn NMR (CDCl₃, ppm): δ 146.50.

4.2.7. $[(\text{Bu}_3\text{Sn})_2(m\text{-CDC})(4,4'\text{-vinylenedipyridine})]_n$ (**7**)

A mixture of 0.10 mmol (*n*-Bu₃Sn)₂O, *m*-CDCH₂ (23.2 mg, 0.10 mmol) and 4,4'-vinylenedipyridine (18.2 mg, 0.10 mmol) was heated under reflux in a mixture of toluene and ethanol (10 ml, *v/v* = 3:2) for 6 h affording a clear solution. The reaction mixture was filtered and the solvent was removed in vacuo to afford a white

Table 7
Crystallographic data and structure refinement parameters for complexes 1–7.

Complex	1	2	3	4	5	6	7
Empirical formula	C ₄₂ H ₄₈ B ₁₀ O ₆ Sn ₂	C ₂₈ H ₄₁ B ₁₀ NO ₄ Sn	C ₁₂₄ H ₁₄₀ B ₃₀ O ₁₈ Sn ₆	C ₁₂ H ₃₆ B ₁₀ O ₆ Sn ₂	C ₂₃ H ₆₃ B ₂₀ NO ₈ Sn ₃	C ₃₈ H ₇₂ B ₁₀ N ₂ O ₄ Sn ₂	C ₂₀ H ₃₇ B ₅ NO ₂ Sn
M	994.28	682.41	2954.80	621.89	1054.01	966.46	496.25
Crystal system	Monoclinic	Trigonal	Monoclinic	Orthorhombic	Triclinic	Triclinic	Monoclinic
Space group	P2(1)/c	R-3	C2/c	Pna2(1)	P-1	P-1	C2/c
a [Å]	21.0601(18)	26.889(3)	20.7520(17)	19.1982(18)	10.6775(10)	9.8105(4)	10.7386(9)
b [Å]	12.5639(12)	26.889(3)	13.4129(11)	20.724(2)	14.3346(15)	9.8194(6)	21.536(2)
c [Å]	7.9351(15)	29.512(3)	49.497(4)	14.0643(13)	17.2197(17)	26.9493(11)	23.474(2)
α [°]	90	90	90	90	70.9890(10)	92.342(4)	90
β [°]	100.8090(10)	90	93.8440(10)	90	88.096(2)	99.540(3)	94.7770(10)
γ [°]	90	120	90	90	77.1150(10)	109.152(5)	90
V [Å ³]	4661.4(7)	18 478(4)	13746.3(19)	5595.7(9)	2426.9(4)	2405.8(2)	5409.8(9)
Z	4	18	4	8	2	2	8
D _{calc} (Mg/m ³)	1.417	1.104	1.428	1.476	1.442	1.334	1.219
μ [mm ⁻¹]	1.115	0.650	1.134	1.807	1.570	1.075	0.958
F(000)	1992	6264	5912	2448	1044	992	2040
Crystal size (mm)	0.48 × 0.26 × 0.17	0.45 × 0.42 × 0.39	0.45 × 0.22 × 0.21	0.30 × 0.21 × 0.18	0.41 × 0.32 × 0.15	0.32 × 0.28 × 0.21	0.39 × 0.22 × 0.19
Reflections collected	22 918	38 838	34 812	28 253	12 347	17 211	13 430
Independent reflections	8202	7192	12 057	9774	8414	8502	4757
R _{int}	0.0431	0.0632	0.0677	0.0698	0.0507	0.0481	0.0500
Goodness-of-fit on F ²	1.057	0.858	1.149	1.078	1.017	1.081	1.096
R ₁ [I > 2σ(I)], R ₁ (all data)	0.0637, 0.1802	0.0654, 0.1561	0.0997, 0.1953	0.0836, 0.2169	0.0723, 0.1929	0.0592, 0.1419	0.0650, 0.1853
wR ₂ [I > 2σ(I)], wR ₂ (all data)	0.1086, 0.2337	0.1027, 0.1817	0.1386, 0.2160	0.1649, 0.2725	0.1032, 0.2171	0.0753, 0.1532	0.1146, 0.2424

solid product. The light red single crystals of **7** were obtained by the slow evaporation of CH₃CN/Acetone solution of product. Yield: 79%. M.P. 149–151 °C. Anal. Calc. for C₂₀H₃₇B₅NO₂Sn: C 48.40, H 7.51, N 2.82%; Found: C 48.10, H 7.62, N 2.62%. IR (KBr, cm⁻¹): ν_{as}(COO), 1662.7; ν_s(COO), 1337.6; ν(Sn–C), 545.0; ν(Sn–O), 467.1, ν(Sn–N), 452.1. ¹H NMR (CDCl₃, ppm): δ 7.26 (s, 1H, –CH=CH–), 7.40 (d, 2H, bpe), 8.63 (d, 2H, bpe), 0.87–0.90 (t, 9H, butyl CH₃), 1.24–1.34 (m, 6H, butyl –CH₂–), 1.57–1.74 (b, 12H, butyl Sn–CH₂–CH₂–). ¹³C NMR (CDCl₃, ppm): δ 165.80 (COO); 13.83, 17.20, 27.03, 27.75 (butyl–C), 46.16; 76.80, 76.90 (C-1 and C-7); 150.57, 143.66, 130.78, 121.39 (bpe–C). ¹¹⁹Sn NMR (CDCl₃, ppm): δ 143.41.

4.3. X-ray crystallography studies

The crystals of complexes **1–7** were mounted in Lindemann capillaries under nitrogen. Diffraction data were collected with a Bruker Smart CCD area detector with graphite-monochromated Mo Kα radiation (λ = 0.71073 Å). A semiempirical absorption correction was applied to the data. The structure was solved by direct methods using SHELXS-97 and refined against F² by full-matrix least-squares using SHELXS-97. Hydrogen atoms were placed in calculated positions. Crystal data and experimental details of the structure determinations are listed in Table 7.

4.4. Pharmacology

4.4.1. Cell lines and culture conditions

The human tumor cell lines, chronic myeloid leukemia cell line (K-562) and cervical cancer cell line (Hela), which were used for screening, were grown and maintained in RPMI-1640 and MEM medium, respectively, supplemented with 10% fetal bovine serum at 37 °C in humidified incubators in an atmosphere of 5% CO₂.

4.4.2. Cytotoxicity assays

K-562 and Hela cell proliferation in compound-treated cultures were evaluated by using a system based on the tetrazolium compound (MTT) and sulforhodamine B (SRB) methods, respectively, in the School of Medicine and Pharmacy, Ocean University of China. K-562 cell lines (90 μl) were seeded into 96 well plates at a concentration of about 10 000–15 000 cells/mL and were incubated in an atmosphere of 5% CO₂ for 24 h. Then, 10 μl of the sample (organotin

complexes) DMSO solution was added and further incubation was carried out at 37 °C for 48 h. The compounds were serially diluted (in four to six steps) with DMSO and added to cell incubation medium at the final concentration of 0.1 μM DMSO in the medium. 20 μl of 5 mg/mL of MTT mixture was added to each well. After 4 h incubation, the culture medium was removed, and 50 μl of isopropanol was added to dissolve the insoluble blue formazan precipitates produced by MTT reduction. The plate was shaken for 20 min on a plate shaker to ensure complete dissolution. The optical density of each well was measured at 570 nm wavelength. The cytotoxic activity was determined three times in independent experiments.

Hela cell lines (90 μl) were seeded into 96 well plates at a concentration of about 10 000–15 000 cells/ml and were incubated in an atmosphere of 5% CO₂ for 24 h. Then 10 μl of tested agents either complete culture medium (control wells) or drug concentrations diluted in complete culture medium (test wells) was added and further incubation was carried out at 37 °C for 48 h. Drug cytotoxic was measured by means of SRB colorimetric assay. Culture medium was removed via downward tapping and 10% cold (4 °C) trichloroacetic acid (TCA) was gently added to the wells. Microplates were left for 30 min at 4 °C, washed five times with tap water and left to dry at room temperature for at least 24 h. Subsequently, 100 μl of 4 mg/ml sulforhodamine B in 1% acetic acid solution was added to each well and left at room temperature for 20 min. SRB was removed and the plates were washed five times with 1% acetic acid before air drying. Bound SRB was solubilized with 150 μl of unbuffered Tris-base solution and plates were left on a plate shaker for at least 10 min. The optical density of each well was measured at 515 nm wavelength. The cytotoxic activity was determined three times in independent experiments.

Acknowledgments

The authors thank the National Natural Science Foundation of China (20971063) for financial supported.

Appendix A. Supplementary material

CCDC 8533849 (**1**), 889839 (**2**), 889840 (**3**), 889842 (**4**), 889841 (**5**), 889843 (**6**) and 889844 (**7**) contain the supplementary

crystallographic data for this paper. These data can be obtained free of charge from The Cambridge Crystallographic Data Centre via www.ccdc.cam.ac.uk/data_request/cif.

Appendix B. Supplementary material

Supplementary data related to this article can be found at <http://dx.doi.org/10.1016/j.jorganchem.2013.04.039>.

References

- [1] G. Gasser, I. Ott, N. Metzler-Nolte, *J. Med. Chem.* 54 (2010) 3–25.
- [2] I. Ott, R. Gust, *Arch. Pharm. Chem. Life Sci.* 340 (2007) 117–126.
- [3] S.H. VanRijt, P. Sadler, *Drug Discov. Today* 14 (2009) 1089–1097.
- [4] V. Chandrasekhar, S. Nagendran, V. Baskar, *Coord. Chem. Rev.* 235 (2002) 1–52.
- [5] X.Q. Song, A. Zapata, G. Eng, *J. Organomet. Chem.* 691 (2006) 1756–1760.
- [6] N. Gerasimchuk, T. Maher, *Inorg. Chem.* 46 (2007) 7268–7284.
- [7] H.D. Yin, C.H. Yue, M. Hong, J.C. Cui, Q.K. Wu, X.Y. Zhang, *Eur. J. Med. Chem.* 58 (2010) 533–542.
- [8] Y. Byun, J. Yan, A.S. Al-Madhoun, J. Johnsamuel, W. Yang, R.F. Barth, S. Eriksson, W. Tjarks, *J. Med. Chem.* 48 (2005) 1188–1198.
- [9] J.F. Valliant, K.J. Guenther, A.S. King, P. Morel, P. Schaffer, O.O. Sogbein, K.A. Stephenson, *Coord. Chem. Rev.* 232 (2002) 173–230.
- [10] I.B. Sivaev, V.I. Bregadze, N.T. Kuznetsov, *Russ. Chem. Bull.* 51 (2002) 1362–1374.
- [11] M.F. Hawthorne, A. Maderna, *Chem. Rev.* 99 (1999) 3421–3434.
- [12] I.H. Hall, C.O. Starnes, B.F. Spielvogel, P. Wisian-Neilson, M.K. Das, L. Wojnowich, *J. Pharm. Sci.* 68 (1979) 685–688.
- [13] I.H. Hall, C.J. Gilbert, A.T. McPhail, K.W. Morse, K. Hassett, B.F. Spielvogel, *J. Pharm. Sci.* 74 (1985) 755–758.
- [14] B.F. Spielvogel, A. Sood, I.H. Hall, R.G. Fairchild, P.L. Micca, *Strahlenther. Onkol.* 165 (1989) 123–125.
- [15] I.H. Hall, A. Elkins, W.J. Powell, S. Karthikeyan, A. Sood, B.F. Spielvogel, *Anti-cancer Res.* 18 (1998) 2617.
- [16] I.H. Hall, B.F. Spielvogel, A.T. McPhail, *J. Pharm. Sci.* 73 (1984) 973–977.
- [17] M.C. Miller III, J.R. Vance, K.F. Bastow, A. Sood, B.F. Spielvogel, I.H. Hall, *Met. Based Drugs* 4 (1997) 229–241.
- [18] M.C. Miller III, A. Sood, B.F. Spielvogel, R.P. Shrewsbury, I.H. Hall, *Met. Based Drugs* 3 (1996) 219–226.
- [19] C.K. Sood, A. Sood, B.F. Spielvogel, J.A. Yousef, B.S. Burnham, I.H. Hall, *J. Pharm. Sci.* 80 (1991) 1133–1140.
- [20] V.I. Bregadze, S.A. Glazun, P.V. Petrovskii, Z.A. Starikova, V.A. Rochev, H. Dalil, M. Biesemans, R. Willem, M. Gielen, D. de Vos, *Appl. Organomet. Chem.* 17 (2003) 453–457.
- [21] V.I. Bregadze, S.A. Glazun, P.V. Petrovskii, Z.A. Starikova, A.G. Buyanovskaya, R.U. Takazova, M. Gielen, D. de Vos, M. Kemmer, M. Biesemans, R. Willem, *Appl. Organomet. Chem.* 18 (2004) 191–194.
- [22] M. Gielen, A. Bouhdid, R. Willem, V.I. Bregadze, L.V. Ermanson, E.R.T. Tiekink, *J. Organomet. Chem.* 501 (1995) 277–281.
- [23] E.R.T. Tiekink, M. Gielen, A. Bouhdid, R. Willem, V.I. Bregadze, L.V. Ermanson, S.A. Glazun, *Met. Based Drugs* 4 (1997) 75–80.
- [24] V.I. Bregadze, *Chem. Rev.* 92 (1992) 209–223.
- [25] G.K. Sandhu, R. Hundal, *J. Organomet. Chem.* 412 (1991) 31–38.
- [26] T.S.B. Baul, C. Masharing, S. Basu, E. Rivarola, M. Holcápek, R. Jirásko, A. Lyčka, D. de Vos, A. Linden, *J. Organomet. Chem.* 691 (2006) 952–965.
- [27] V. Chandrasekhar, C. Mohapatra, R.J. Butcher, *Crystal Growth Des.* 12 (2012) 3285–3295.
- [28] R. García-Zarracino, H. Hopfl, *J. Am. Chem. Soc.* 127 (2005) 3120–3130.
- [29] C.L. Ma, J.K. Li, R.F. Zhang, D.Q. Wang, *J. Organomet. Chem.* 691 (2006) 1713–1721.
- [30] C.L. Ma, B.Y. Zhang, S.L. Zhang, R.F. Zhang, *J. Organomet. Chem.* 696 (2011) 2165–2171.
- [31] T.S.B. Baul, C. Masharing, G. Ruisi, R. Jirásko, M. Holcápek, D. de Vos, D. Wolstenholme, A. Linden, *J. Organomet. Chem.* 692 (2007) 4849–4862.
- [32] R.G. Swisher, J.F. Vollano, V. Chandrasekhar, R.O. Day, R.R. Holmes, *Inorg. Chem.* 23 (1984) 3147–3152.
- [33] J.F. Vollano, R.O. Day, D.N. Rau, V. Chandrasekhar, R.R. Holmes, *Inorg. Chem.* 23 (1984) 3153–3160.
- [34] V. Chandrasekhar, R. Thirumoorathi, *Dalton Trans.* 39 (2010) 2684–2691.
- [35] D.Y. Zhang, Z.Y. Li, L.Y. Shi, X.M. Wu, W.Y. Hua, *Chin. J. Org. Chem.* 28 (2008) 1911–1917.
- [36] R.Q. Pang, L. Wang, J. Chen, et al., *Chin. J. Clin. Oncol.* 8 (2003) 332–334.
- [37] D. Tzimopoulos, I. Sanidas, A.-C. Varvogli, A. Czapik, M. Gdaniec, E. Nikolakaki, P.D. Akrivos, *J. Inorg. Biochem.* 104 (2010) 423–430.
- [38] A.M. Pizarro, A. Hablemariam, P.J. Sadle, *Activation Mechanisms for Organometallic Anticancer Complexes*, in: G. Jaouen, N. Metzler-Nolte (Eds.), *Med. Organomet. Chem. Topics in Organomet. Chem.*, 32, 2010, pp. 21–46.
- [39] X.Q. Song, G.Y. Zhong, Y.Q. Huang, *Chin. J. Org. Chem.* 22 (2002) 735–740.
- [40] S.B. Kahl, R.A. Kasar, *J. Am. Chem. Soc.* 118 (1996) 1223–1224.